

THE LOW-SPIN BLACK HOLE IN LMC X-3

JAMES F. STEINER^{1†}, JEFFREY E. MCCLINTOCK¹, JEROME A. OROSZ², RONALD A. REMILLARD³,
CHARLES D. BAILYN⁴, MARI KOLEHMAINEN⁵, ODELE STRAUB⁶

Draft version October 12, 2018

ABSTRACT

Building upon a new dynamical model for the X-ray binary LMC X-3, we measure the spin of its black hole primary via the continuum-fitting method. We consider over one thousand thermal-state *RXTE* X-ray spectra of LMC X-3. Using a large subset of these spectra, we constrain the spin parameter of the black hole to be $a_* = 0.21_{-0.22}^{+0.18}$ (90% confidence). Our estimate of the uncertainty in a_* takes into account a wide range of systematic errors. The low spin and low mass of the black hole further align LMC X-3 with the class of Roche-lobe overflowing, transient black-hole systems. We discuss evidence for a correlation between a black hole's spin and the complexity of its X-ray spectrum.

Subject headings: accretion, accretion disks — black hole physics — stars: individual (LMC X-3) — X-rays: binaries

1. INTRODUCTION

Leong et al. (1971) discovered LMC X-3 during the first year of the *Uhuru* mission. In 1983, Cowley et al. (1983) showed via dynamical observations that the compact X-ray source in this 1.7-day binary is a black hole. In Orosz et al. (2014) we use new optical data to derive a much-improved dynamical model of the system, which contains a B-type secondary. Of chief importance, Orosz et al. report tight constraints on the orbital inclination angle of the binary, $i = 69.6 \pm 0.6$ deg, and the mass of the black hole, $M = 6.95 \pm 0.33 M_\odot$.

LMC X-3 is unusual compared to the full assemblage of black-hole binary systems: On the one hand, like the transient systems, its X-ray intensity is highly variable because the black hole is fed by Roche-lobe overflow. On the other hand, however, the system almost continually maintains itself in an X-ray bright mode like the persistent (wind-fed) systems (McClintock et al. 2013; Soria et al. 2001).

Transient versus persistent black holes are further set apart by the properties of their black hole primaries: the transient black hole masses are low and tightly distributed ($7.8 M_\odot \pm 1.2 M_\odot$), while the masses of the persistent black holes are appreciably higher ($\gtrsim 11 M_\odot$; Özel et al. 2010). Meanwhile, the spins of the transients are widely distributed ($a_* \approx 0 - 1$), while the three persistent black holes with spin measurements are all high ($a_* \gtrsim 0.85$). The mode of mass transfer firmly identifies LMC X-3 as belonging to the class of transient black hole

binaries. The low mass of LMC X-3's primary and its low spin (reported herein) are perfectly congruent with this classification.

Despite strong variations in X-ray brightness (> 3 orders of magnitude), the X-ray spectrum of LMC X-3 is nearly always in a thermal, disk-dominated state (ideal for measuring spin via the continuum-fitting method), except during occasional prolonged excursions into a low-intensity hard state (e.g., Smale & Boyd 2012; Wilms et al. 2001). Because the X-ray spectrum is strongly disk-dominated, relatively featureless, and minimally affected by interstellar absorption, LMC X-3 is a touchstone for testing spectral models of black-hole accretion disks (e.g., Kubota et al. 2010; Straub et al. 2011). In a precursor to this work, we fitted all archival X-ray spectra with reliable flux calibration to a relativistic model of a thin accretion disk. For hundreds of Rossi X-ray Timing Explorer (*RXTE*) spectra, we showed that the inner radius of the disk is constant to within $\approx 2\%$ over a span of 14 years despite the gross variability of the source. Furthermore, for an ensemble of eight X-ray missions spanning 26 years, we showed that the radius is constant to better than $\approx 6\%$, despite the uncertainties associated with cross-calibrating the various detectors. This result is the strongest observational evidence to date that spin can be reliably inferred by measuring the inner-disk radius.

The elegant simplicity of a black hole is encapsulated in the famous "no-hair theorem", which tells us that an astrophysical black hole is *completely* described by just its mass and spin angular momentum (the third parameter, electrical charge, being effectively neutral in astrophysical settings). A spinning black hole is an enormous capacitor of angular momentum, with the spin as a ready energy source that can be tapped mechanically in a black hole's ergosphere. Spin has long been proposed as the likely energy source behind the enormously energetic jets emitted from black holes (e.g., Blandford & Znajek 1977). This assumption has gained recent support both theoretically (e.g., Tchekhovskoy et al. 2011), and observation-

jsteiner@cfa.harvard.edu

¹ Harvard-Smithsonian Center for Astrophysics, 60 Garden Street, Cambridge, MA 02138.

² Department of Astronomy, San Diego State University, 5500 Campanile Drive, San Diego, CA 92182.

³ MIT Kavli Institute for Astrophysics and Space Research, MIT, 70 Vassar Street, Cambridge, MA 02139.

⁴ Astronomy Department, Yale University, P.O. Box 208101, New Haven, CT 06520.

⁵ Astrophysics, Department of Physics, University of Oxford, Keble Road, Oxford OX1 3RH, UK.

⁶ LUTH, Observatoire de Paris, CNRS, Université Paris Diderot, 5 place Jules Janssen, 92190 Meudon, France.

[†] Hubble Fellow.

ally (Narayan & McClintock 2012; Steiner et al. 2013; McClintock et al. 2013, but see Russell et al. 2013).

The two primary means by which black hole spins are measured are 1) X-ray continuum-fitting (Zhang et al. 1997), and 2) modeling relativistic reflection (frequently termed the “Fe-line” method) (Fabian et al. 1989). The single precept which underpins both methods is the monotonic relationship between spin and the radius of the innermost-stable circular orbit (ISCO) for particles orbiting the black hole. Consequently, by determining R_{ISCO} , which is presumed to be the inner-radius of the accretion disk, one may directly infer a black hole’s angular momentum J , usually expressed as the dimensionless spin parameter,

$$a_* \equiv cJ/GM^2, \quad 0 \leq |a_*| \leq 1. \quad (1)$$

The continuum-fitting method – the basis for the work presented here – has been used to estimate the spins of roughly a dozen stellar-mass black holes (e.g., McClintock et al. 2013, and references therein, Middleton et al. 2006; Kolehmainen et al. 2011). In this method, the inner-disk radius is estimated using the thermal, multicolor blackbody continuum emission from the disk (e.g., Novikov & Thorne 1973; Shakura & Sunyaev 1973). The Fe-line method measures R_{in} using the redward extent of relativistic broadening of reflection features in the disk, and has been applied just as widely (e.g., Brenneman & Reynolds 2006; Walton et al. 2012; Reis et al. 2013 and Reynolds 2013 and references therein). Both methods, but especially the Fe-line method, are also being applied to measure the spins of supermassive black holes in active galactic nuclei (AGN). LMC X-3 is ideal for continuum-fitting as it offers a strong, dominantly thermal continuum at nearly all times. However, its spectra accordingly contain very little signal in reflection, and so reflection models cannot constrain spin for this source.

Prior to this investigation, a preliminary estimate of LMC X-3’s spin was obtained via a continuum-fitting measurement from a single *BeppoSAX* spectrum by Davis et al. (2006), later bolstered by Kubota et al. (2010). Their results were hampered primarily by the poorly constrained mass available at the time, and so only a rough estimate was possible, $a_* \sim 0.3$. Employing the new and precise mass measurement from Orosz et al. (2014), we revisit LMC X-3’s spin determination. Using the largest data set available to us – over a decade of pointed monitoring with (*RXTE*) – we estimate the spin and its uncertainty for LMC X-3 via X-ray continuum fitting.

2. DATA AND ANALYSIS

We replicate the reduction and analysis techniques adopted in Steiner et al. (2010) while considering the *full* set of *RXTE* pointed observations over the mission lifetime. To ensure the most consistent analysis, we only use data for the PCU-2 detector, which has the most stable calibration and was most frequently active. We separate and analyze each segment of continuous exposure, applying a 300 s lower limit. For very long observations, we divide the interval into segments with individual exposure times less than 5000 s. In total, this yields 1598 spectra with an average exposure time and net signal of

~ 2 ks and $\sim 50 \times 10^3$ counts, respectively. The spectra have been background subtracted and corrected for detector dead time.

We fit the data over the energy range 2.8–25 keV and include a 1% systematic error in the count rates in each channel to account for uncertainties in the response of the detector. We use the average PCU-2 spectrum of the Crab to establish our standard absolute flux calibration (Toor & Seward 1974)⁸. For this step, we use the model CRABCOR (Steiner et al. 2010) which rescales the normalization by 9.7% and adjusts the spectral index by $\Delta\Gamma = 0.01$. There is relatively little interstellar absorption, $N_{\text{H}} = 4 \times 10^{20} \text{ cm}^{-2}$ (Page et al. 2003), which is kept fixed during fitting and modeled via TBABS (Wilms et al. 2000).

Errors are everywhere quoted at the 1σ level unless otherwise indicated. For the primary – i.e., thermal disk – component of emission, we use KERRBB2 (McClintock et al. 2013; Davis & Hubeny 2006; Li et al. 2005), which incorporates all relativistic effects and directly solves for spin. The model KERRBB2 assumes that the disk is razor thin and optically thick. To apply KERRBB2 one must specify four external input parameters: black hole mass, disk inclination, distance D and the viscosity parameter α (Shakura & Sunyaev 1973). The Compton power-law component is modeled empirically using SIMPL (Steiner et al. 2009b). Our complete spectral model is expressed as TBABS(SIMPL \otimes KERRBB2) \times CRABCOR.

As an initial step in the analysis, we fit the full data set to our spectral model using fiducial values for M and i (Section 1) and a distance $D = 48.1 \pm 2.2$ kpc (Orosz et al. 2009), and adopting a viscosity $\alpha = 0.03$. We include limb darkening and returning radiation effects, adopt zero torque at the inner-disk boundary, and make the standard assumption that the black hole’s spin axis is aligned with the orbital angular momentum (Steiner & McClintock 2012; McClintock et al. 2013). There are just four free fit parameters: a_* , mass accretion rate \dot{M} , photon spectral index Γ , and the scattering fraction f_{SC} (the fraction of disk photons scattered in the corona). We constrained the photon index to lie in the range $\Gamma = 1.5 - 3.5$; the three other parameters are unconstrained.

Subsequent to fitting all of the spectra, we use our initial results to screen out spectra that are unsuitable for the measurement of spin: We reject data for which f_{SC} exceeds 25% (141/1598; see Steiner et al. 2009a). We likewise discard data for which the goodness-of-fit $\chi^2_{\nu} > 2$ (4/1598), arriving at a sample of 1454 thermal-state spectra. Figure 1 shows a fit to one representative spectrum. The thermal component in red plainly dominates the flux, and our model of a featureless Comptonized disk provides a more-than sufficient fit ($\chi^2_{\nu} \approx 0.5$), with only four free parameters.

A restriction of KERRBB2 is that it is only applicable to those data firmly in the “thin-disk” limit (scale height $H/R \ll 1$). The scale-height of the X-ray emitting region of the disk is determined by radiation pressure, itself set by the luminosity. Previous work has demonstrated

⁸ We have explored the effects of the variability of the Crab’s spectrum (Wilson-Hodge et al. 2011) on our results and find that they are negligible.

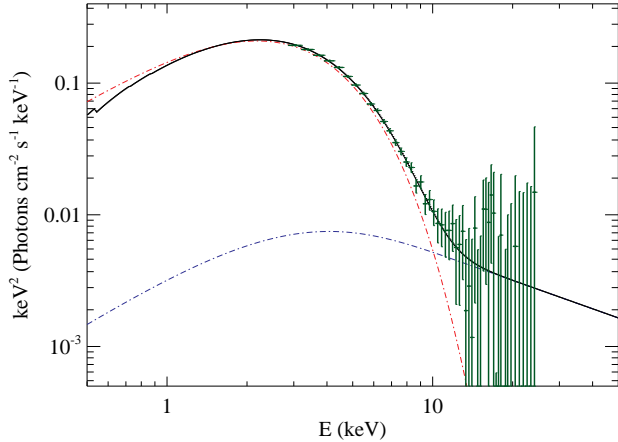


FIG. 1.— A representative fit to a 4 ks exposure of LMC X-3 from 9 December 1998. The black line shows the composite model, including the effects of photoelectric absorption. The red and blue dash-dotted lines show the intrinsic thermal disk and power-law components, respectively.

that the presence of a geometrically-thin, optically-thick disk can be reliably assumed over the luminosity range $L \approx 5 - 30\% L_{\text{Edd}}$, where the Eddington-luminosity $L_{\text{Edd}} \approx 1.3 \times 10^{38} (M/M_{\odot}) \text{ erg s}^{-1}$ (McClintock et al. 2013).

3. RESULTS

In our initial run, a total of 391 spectra fulfilling the thermal selection also match this luminosity (thin-disk) criterion. Using the spectra which make both cuts, we obtain a spin $a_* = 0.190 \pm 0.005$ (weighted mean and its 1σ error).

A comprehensive run is now performed to assess the error in spin from uncertainties in the other measurement quantities. For each point along a grid of M , i , and D , we repeat our spectral fits to the pre-selection of 1454 spectra. Mass is sampled from $M : 5 - 11 M_{\odot}$, inclination $i : 60^\circ - 75^\circ$, and $D : 41 - 56 \text{ kpc}$. The values of L/L_{Edd} depend upon M , i , and D , but typically ~ 400 of these spectra fulfill the luminosity criterion. At *each* gridpoint, the distribution of spin from the selected spectra gives a single, mean spin, and its uncertainty⁹. By applying weights according to the probability of each gridpoint (calculated using the measurements of M , i , and D given in Sections 1,2), results are combined to achieve a composite distribution in spin. This distribution is inclusive of *all measurement errors*.

In previous work, we have assessed the effects of a wide range of systematic errors (Steiner et al. 2010, 2011) and found that only two are significant: the uncertainty in α and the uncertainty in the spectrum of the Crab, which we use as our flux standard (Section 2). We take uncertainty in α into account by repeating the analysis for $\alpha = 0.01$ and $\alpha = 0.1$ and then averaging the spin distributions, weighting them equally. We incorporate a 10% uncertainty in the absolute X-ray flux calibration

⁹ As demonstrated in Steiner et al. (2010), the inner disk radius (which corresponds to a particular value of spin) at any grid point has a spread of $< 5\%$, while the mean of the distribution is determined with much greater precision.

TABLE 1
FINAL SPIN DETERMINATION

| Confidence Level | Spin Interval | R_{in} Interval |
|---------------------|------------------------|---------------------------------|
| 68% (1σ) | $a_* = 0.21 \pm 0.12$ | $R_{\text{in}}/M = 5.3 \pm 0.4$ |
| 90% | $0.21^{+0.18}_{-0.22}$ | $5.3^{+0.7}_{-0.6}$ |
| 95% (2σ) | $0.21^{+0.21}_{-0.27}$ | $5.3^{+0.9}_{-0.8}$ |
| 99.7% (3σ) | $0.21^{+0.30}_{-0.44}$ | $5.3^{+1.4}_{-1.1}$ |

NOTE. — Incremental confidence intervals for our final, adopted spin result, which accounts for all sources of error.

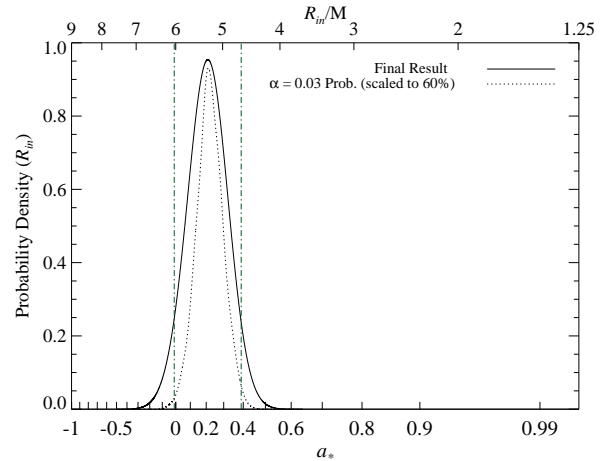


FIG. 2.— The net probability distribution of a_* (R_{in}). The abscissa is scaled logarithmically in R_{in} , a metric which reflects our measurement scale. The corresponding quantity of chief physical interest, namely a_* , is shown on the lower axis. Our final distribution (solid line) incorporates measurement error and systematic error, most notably uncertainties in the α -viscosity and the absolute flux calibration. The pair of dash-dotted lines indicate the 90% confidence interval. The dotted line shows our result for $\alpha = 0.03$ ignoring the effects of systematic error (where the probability distribution has been rescaled for comparison).

(Toor & Seward 1974) by broadening our distribution in R_{in} using a Gaussian kernel with 5% width. Finally, an additional 2% broadening is used to account for the small variation introduced by adopting a different choice of Comptonization model (Steiner et al. 2010).

The combined result is shown in Figure 2. Our *final* measurement of spin, including all measurement *and* systematic uncertainties is $a_* = 0.21^{+0.18}_{-0.22}$ (90%). For comparison, our measurement without considering systematic errors (using $\alpha = 0.03$) yielded $a_* = 0.21 \pm 0.10$ (90%). Table 1 gives our final determination of spin as measured at several confidence levels, explicitly given because the measurement errors in spin are generally non-linear.

As a bottom line, LMC X-3 has a precisely determined spin, which is low.

4. DISCUSSION

In Section 3 we considered the effects of all measurement errors and known systematic errors on our estimate of a_* (apart from the assumption that the black hole's spin is aligned with the orbital angular momentum vector; see Section 5.4 in McClintock et al. 2013). In this section we consider the error we incur by our reliance on

the Novikov-Thorne model and conclude that it is relatively small. We then compare the low spin of LMC X-3 to the spins of several other sources, tentatively concluding that the Compton component is relatively weak for low spin black holes and strong for rapidly spinning ones.

4.1. Errors from the Novikov-Thorne Model

While our earlier study of LMC X-3 (Steiner et al. 2010), and similar studies of other black hole binaries (e.g., Gierliński & Done 2004), provide compelling evidence that the inner disk radius is constant in black hole binaries, it does not prove that this radius is in fact R_{ISCO} . The central assumption of the thin-disk model is that the viscous torque vanishes at the ISCO and that no flux is emitted from within this radius. This assumption has been tested by several groups using sophisticated general-relativistic magnetohydrodynamic (GRMHD) codes. The results from two groups are exemplified by three key studies, each aimed at testing the reliability of spin estimates. Results from one group are reported in Noble et al. (2011), and from the other in Kulkarni et al. (2011) and Zhu et al. (2012). Both groups produce synthetic observations of their simulations as they would appear to a distant observer at a range of viewing angles.

Although there are subtle differences in the approaches taken by the two groups, one can make a reasonably direct comparison between Kulkarni et al. (2011) and Noble et al. (2011). Both groups used ad hoc but reasonable cooling prescriptions in post-processing to convert magnetic stresses into radiation. By treating the dissipation as local and thermal, disk spectra have been generated for a nonspinning black hole by Noble et al. and for black holes with a range of spins by Kulkarni et al. From these two works, one concludes that spin measurements systematically *overestimate* the spin, that this effect is most pronounced at high inclination, and that the fractional change in R_{in} is independent of a_* . The deviation of $R_{\text{in}}/R_{\text{ISCO}}$ from unity is of order ten percent. However, the state-of-the-art analysis has been achieved by Zhu et al. (2012), and its findings differ appreciably, as we now discuss.

Zhu et al. include, as an additional post-processing step, full radiative-transfer through the disk atmosphere in generating the simulated GRMHD spectra. In contrast to the $\sim 10\%$ shift in $R_{\text{in}}/R_{\text{ISCO}}$ reported by Kulkarni et al. (2011) and Noble et al. (2011), Zhu et al. find a much smaller deviation because their more sophisticated approach identifies a hard power-law component of emission that is largely produced inside R_{ISCO} . It is this component, which in the earlier work was lumped in with the thermal emission, that was largely responsible for the shift in $R_{\text{in}}/R_{\text{ISCO}}$. Analyzing their simulated spectra using the model in Section 2, Zhu et al. find that the shift in $R_{\text{in}}/R_{\text{ISCO}}$ is only $\sim 3\% \pm 2\%$ and that it depends only weakly on inclination, α , and luminosity (see Table 2 in Zhu et al. 2012).

In short, deviations from Novikov-Thorne are likely of minor consequence. For the nominal spin of LMC X-3, a 3% offset in R_{in} would imply $a_* \approx 0.16$ (a shift of $\Delta a_* = -0.05$), or a 0.4σ correction to our final result.

4.2. A Possible Link Between Spin and Spectral Complexity

Although the spins of more than a dozen stellar-mass black holes have been measured, only two have spins as low as LMC X-3, namely, A0620-00 and H1743-322 (McClintock et al. 2013). The spectra of A0620-00 and LMC X-3 (at luminosities $> 0.05L_{\text{Edd}}$) are remarkably simple, consisting of a dominant thermal component with Compton power-law and reflection components that are always quite faint. The spectrum of H1743-322 is not as consistently simple. However, for a large sample of 65 thermal spectra, the Compton (and reflection) component of this source is very faint with a mean strength of $f_{\text{SC}} = 1.2\%$ (Steiner et al. 2009a), weaker than for any other sources with a spin measurement (apart from A0260-00 and LMC X-3).

The simplicity of the spectra of these three sources contrasts sharply with the spectra of the two extreme-spin sources, Cyg X-1 and GRS 1915+105 (McClintock et al. 2013, and references therein), and to a lesser degree the spectrum of LMC X-1 ($a_* = 0.92_{-0.07}^{+0.05}$; Gou et al. 2009). The spectra of these sources are generally complex; i.e., they show strong rms variability (from their power-density spectra), are strongly Comptonized, and contain prominent reflection features. Comparison with the simple spectra of A0620-00, LMC X-3 and H1743-322 suggests that spectral complexity is correlated with spin.

A prediction of this hypothesis is that the spin of GS 2000+25, whose spectral properties (and outburst light curve) are very similar to that of A0620-00 (Terada et al. 2002), is very low, and that the spin of V404 Cyg, whose spectrum was consistently observed to be strongly Comptonized (Tanaka & Lewin 1995), is quite high. One other source may be able to provide a strong test of our prediction: 4U1957+11. Although the spin and mass are presently unknown, there are indications that the former is likely high and the latter likely low (Nowak et al. 2012), while its spectrum is very thermal and generally only weakly Comptonized. Confirmation of an extreme spin for 4U 1957+11 could decisively rule out this hypothesis.

5. CONCLUSIONS

We have analyzed all 1598 spectra of LMC X-3 collected during the *RXTE* mission. Using a selected sample of ≈ 400 spectra, our precise measurement of black hole mass and inclination (Orosz et al. 2014), and the continuum-fitting method, we derive a strong constraint on the spin of the black hole: $a_* = 0.21_{-0.22}^{+0.18}$ (90% confidence). Our comprehensive error estimate takes into account all known sources of uncertainty, e.g., the uncertainties in M , i , D , α , and in the absolute X-ray flux calibration.

The simple and predominately thermal spectra of LMC X-3 and A0620-00, the black holes with the lowest measured spins, contrast sharply with the complex and strongly Comptonized spectra of GRS 1915+105 and Cyg X-1, the two black holes with near-extreme spin. This comparison suggests a possible link between spin and the degree of spectral complexity, a hypothesis that can be tested, and which predicts a low spin for GS 2000+25 and a high spin for V404 Cyg. The black hole 4U 1957+11 may allow a falsification of the hypothesis, if its spin can be measured.

By virtue of the no-hair theorem, we have a complete and quite precise description of the black hole in LMC X-3. These three – and only three – characteristics define the black hole in entirety: a charge of zero, $M \approx 7.0 M_{\odot}$ and $a_* \approx 0.2$.

This work was made possible by the Odyssey computing cluster, supported by the FAS Science Division

Research Computing Group at Harvard University. We thank Chris Done for enlivening discussions on LMC X-3 and Colleen Hodge-Wilson for providing data on the Crab's variability. Support for JEM has been provided by NASA grant NNX11AD08G, and for JFS by NASA Hubble Fellowship grant HST-HF-51315.01.

Facility: RXTE

REFERENCES

- Blandford, R. D., & Znajek, R. L. 1977, MNRAS, 179, 433
 Brenneman, L. W., & Reynolds, C. S. 2006, ApJ, 652, 1028
 Cowley, A. P., Crampton, D., Hutchings, J. B., Remillard, R., & Penfold, J. E. 1983, ApJ, 272, 118
 Davis, S. W., Done, C., & Blaes, O. M. 2006, ApJ, 647, 525
 Davis, S. W., & Hubeny, I. 2006, ApJS, 164, 530
 Fabian, A. C., Rees, M. J., Stella, L., & White, N. E. 1989, MNRAS, 238, 729
 Gierliński, M., & Done, C. 2004, MNRAS, 349, L7
 Gou, L., McClintock, J. E., Steiner, J. F., Narayan, R., Cantrell, A. G., Bailyn, C. D., & Orosz, J. A. 2010, ApJ, 718, L122
 Gou, L. J., et al. 2009, ApJ, 701, 1076
 Kolehmainen, M., Done, C., & Díaz Trigo, M. 2011, MNRAS, 416, 311
 Kubota, A., Done, C., Davis, S. W., Dotani, T., Mizuno, T., & Ueda, Y. 2010, ApJ, 714, 860
 Kulkarni, A. K., et al. 2011, MNRAS, 414, 1183
 Leong, C., Kellogg, E., Gursky, H., Tananbaum, H., & Giacconi, R. 1971, ApJ, 170, L67
 Li, L.-X., Zimmerman, E. R., Narayan, R., & McClintock, J. E. 2005, ApJS, 157, 335
 McClintock, J. E., Narayan, R., & Steiner, J. F. 2013, Space Sci. Rev.
 Middleton, M., Done, C., Gierliński, M., & Davis, S. W. 2006, MNRAS, 373, 1004
 Narayan, R., & McClintock, J. E. 2012, MNRAS, 419, L69
 Noble, S. C., Krolik, J. H., Schnittman, J. D., & Hawley, J. F. 2011, ApJ, 743, 115
 Novikov, I. D., & Thorne, K. S. 1973, in Black Holes (Les Astres Occlus), 343–450
 Nowak, M. A., Wilms, J., Pottschmidt, K., Schulz, N., Maitra, D., & Miller, J. 2012, ApJ, 744, 107
 Orosz, J. A., et al. 2009, ApJ, 697, 573
 Orosz, J. A., Steiner, J. F., McClintock, J. E., Buxton, M. M., Bailyn, C. D., Steeghs, D., Torres, M. A. P., & Guberman, A. 2014, ApJ, submitted
 Özel, F., Psaltis, D., Narayan, R., & McClintock, J. E. 2010, ApJ, 725, 1918
 Page, M. J., Soria, R., Wu, K., Mason, K. O., Cordova, F. A., & Priedhorsky, W. C. 2003, MNRAS, 345, 639
 Reis, R. C., Reynolds, M. T., Miller, J. M., Walton, D. J., Maitra, D., King, A., & Degenaar, N. 2013, ArXiv e-prints
 Reynolds, C. S. 2013, Space Sci. Rev.
 Russell, D. M., Gallo, E., & Fender, R. P. 2013, MNRAS, 431, 405
 Shakura, N. I., & Sunyaev, R. A. 1973, A&A, 24, 337
 Smale, A. P., & Boyd, P. T. 2012, ApJ, 756, 146
 Soria, R., Wu, K., Page, M. J., & Sakellou, I. 2001, A&A, 365, L273
 Steiner, J. F., & McClintock, J. E. 2012, ApJ, 745, 136
 Steiner, J. F., McClintock, J. E., & Narayan, R. 2013, ApJ, 762, 104
 Steiner, J. F., McClintock, J. E., & Reid, M. J. 2012, ApJ, 745, L7
 Steiner, J. F., McClintock, J. E., Remillard, R. A., Gou, L., Yamada, S., & Narayan, R. 2010, ApJ, 718, L117
 Steiner, J. F., McClintock, J. E., Remillard, R. A., Narayan, R., & Gou, L. J. 2009a, ApJ, 701, L83
 Steiner, J. F., Narayan, R., McClintock, J. E., & Ebisawa, K. 2009b, PASP, 121, 1279
 Steiner, J. F., et al. 2011, MNRAS, 416, 941
 Straub, O., et al. 2011, A&A, 533, A67
 Tanaka, Y., & Lewin, W. H. G. 1995, in X-ray binaries, p. 126 - 174, ed. W. H. G. Lewin, J. van Paradijs, & E. P. J. van den Heuvel, 126–174
 Tchekhovskoy, A., Narayan, R., & McKinney, J. C. 2011, MNRAS, 418, L79
 Terada, K., Kitamoto, S., Negoro, H., & Iga, S. 2002, PASJ, 54, 609
 Toor, A., & Seward, F. D. 1974, AJ, 79, 995
 Walton, D. J., Reis, R. C., Cackett, E. M., Fabian, A. C., & Miller, J. M. 2012, MNRAS, 422, 2510
 Wilms, J., Allen, A., & McCray, R. 2000, ApJ, 542, 914
 Wilms, J., Nowak, M. A., Pottschmidt, K., Heindl, W. A., Dove, J. B., & Begelman, M. C. 2001, MNRAS, 320, 327
 Wilson-Hodge, C. A., et al. 2011, ApJ, 727, L40
 Zhang, S. N., Cui, W., & Chen, W. 1997, ApJ, 482, L155
 Zhu, Y., Davis, S. W., Narayan, R., Kulkarni, A. K., Penna, R. F., & McClintock, J. E. 2012, MNRAS, 424, 2504